arXiv:1210.1409v1 [astro-ph.CO] 4 Oct 2012

Dark Matter Decay and the Abundance of Ultracompact Minihalos

Yupeng Yang[a,b,c], Guilin Yang[b,c], and Hongshi Zong[b,c]
[a] *Department of Astronomy, Nanjing University, Nanjing*
[b] *Department of Physics, Nanjing University, Nanjing and*
[c] *Joint Center for Particle, Nuclear Physics and Cosmology, Nanjing*

Ultracompact minihalos would be formed if there are larger density perturbations in the earlier epoch. The density of the them is higher comparing with the standard dark matter halos. If the dark matter can decay into the standard particles e.g. photons, these objects would be the potential astrophysical sources. In order to be consistent with the observations, such as *Fermi*, the abundance of ultracompact minihalos must be constrained. On the other hand, the formation of these objects has very tighten relation with the primordial density perturbations on smaller scale, so the fraction of ultracompact minihalos is very important for the modern cosmology. In this work, we investigate the γ-ray signals from ultracompact minihalos due to dark matter decay and research the constraints on the abundance of them in detail for the different parameters.

PACS numbers:

I. INTRODUCTION

The structure formation is one of important field of modern cosmological research. It is well known that the present structures of our observational cosmology come from the earlier density perturbations which produced during the inflation. The amplitude of these density perturbations are $\delta\rho/\rho \sim 10^{-5}$. If the density perturbations at earlier epoch are larger than 0.3 the primordial black holes (PBHs) would be formed [1]. Recently, Ricotti and Gould proposed that if the density perturbations are larger than 10^{-3} [1] but smaller than 0.3, one new kind of dark matter structures named ultracompact minihalos (UCMHs) would be formed [2]. The formation time of these objects is earlier and the density is larger than the standard dark matter halos. If dark matter particles consist of weakly interaction massive particles (WIMP), it is excepted that UCMHs would have notability effect on the cosmological evolution due to the dark matter annihilation or decay. In Refs. [3–5], the authors researched the impact of UCMHs on the cosmological ionization and got the constraints on the abundance of them. If high energy photons are produced by the dark matter annihilation the UCMHs will become one kinds of astrophysical sources and they can contribute the γ-ray background. The authors of Refs. [6–9] investigated these effect and got the constraints on the fraction of UCMHs. Due to the high density of UCMHs, they would be detected by microlensing observations. F. Li et al have researched these effect and also got the constrains on these objects [10]. The formation of UCMHs has very closer relation with the primordial density perturbations on the smaller scale ($k = 5 \sim 10^8\mathrm{Mpc}^{-1}$) which are not constraints by the cosmic microwave background (CMB) [8–10], so the fraction of UCMHs is very important for the modern cosmology. All of the present works mainly focused on the impact of UCMHs due to the dark matter annihilation. Moreover, the fraction of UCMHs obtained by these works are mainly based on the classical parameters of dark matter e.g. $\langle\sigma v\rangle \sim 3 \times 10^{-26}\mathrm{cm}^{-3}\mathrm{s}^{-1}$ and annihilation channel is $b\bar{b}$. In this work, we will research the γ-ray signals from UCMHs due to dark matter decay and investigate the impact of related parameters on their fraction constraints in detail.

---

[1] Actually, this value depends on the rerdshift and the scall of density perturbations, for more details one can see the Ref. [9].

This paper is organized as follows: we show the integrated γ-ray flux from UCMHs due to dark matter decay in Sec. 2. In Sec. 3, we discuss how the related parameters effect the constraints on UCMHs fraction and conclude in Sec. 4.

II. THE γ-RAY SIGNALS FROM UCMHS DUE TO DARK MATTER DECAY

After UCMHs seeded during the radiation dominated epoch, the dark matter particles will be accreted by radial infall. The mass of UCMHs changed slowly until matter dominated. It can be written in the form of [2, 7]

$$M_{\mathrm{UCMHs}}(z) = M_i \left(\frac{1+z_{\mathrm{eq}}}{1+z}\right), \tag{1}$$

where M_i is the mass within the perturbations scale at equality.

The density profile can be obtained through the simulation [2, 11, 12]

$$\rho(r,z) = \frac{3f_{\chi}M_{\mathrm{UCMHs}}(z)}{16\pi R(z)^{\frac{3}{4}}r^{\frac{9}{4}}}, \tag{2}$$

where $R(z) = 0.019\left(\frac{1000}{z+1}\right)\left(\frac{M(z)}{\mathrm{M}_{\odot}}\right)^{\frac{1}{3}}$ pc and $f_{\chi} = \frac{\Omega_{DM}}{\Omega_b+\Omega_{DM}} = 0.83$ [13] is the dark matter fraction which describes that only dark matter content collapsed to form the UCMHs at the beginning. Due to the structure formation effect, the mass of UCMHs will stop increasing at recently and in this work we assume that the corresponding redshift is $z = 10$ [7, 9]. The radius of UCMHs is $R(z = 10) \sim 0.01M_i^{\frac{1}{3}}$ and $R \sim$1 kpc for $M_i = 10^6 M_{\odot}$. So in the following discussions we will also treat UCMHs as point sources [2, 7, 9].

The integrated flux of γ-ray signals from nearby UCMHs can be written as

$$\Phi = \frac{1}{8\pi d^2}\frac{\Gamma}{m_{\chi}}\sum^{i}\int_{E_{th}}^{m_{\chi}} B_{f_i}\frac{dN_i}{dE}dE\int\rho(r)d^3r \tag{3}$$

where the sum is for all decay channels, d is the distance from the Earth. $\frac{dN}{dE}$ is the energy spectrum of dark matter decay and which can be obtained by the public code: DarkSUSY [2]. B_{f_i} is the branch ratio of each decay channel. In this work, we consider every decay channel separately and set $B_f = 1$. The $\mathrm{E_{th}}$ is the threshold value of detector. Here we consider the *Fermi* observation and choose the threshold value $\mathrm{E_{th}} = 100$ MeV. In Fig. 1, the integrated γ-ray signals above 0.1GeV from UCMH are shown. Two decay channels are plotted: $b\bar{b}$ and $\tau^+\tau^-$. For the decay rate, we have chosen $\Gamma = 10^{-26}s^{-1}$ and the distance of UCMH is $d = 10$kpc. In order to comparing with the observations, the point source sensitivity of *Fermi* is also shown [3] ($\Phi_{(\mathrm{E}>100\mathrm{MeV})} = 6.0\times10^{-9}\mathrm{cm}^2\mathrm{s}^{-1}$). From the figure one can see that the integrated flux is proportional to the mass of UCMHs ($\Phi \propto \mathrm{M_{UCMHs}}$) and inversely proportional to the dark matter mass ($\Phi \propto 1/\mathrm{m}_{\chi}$). Actually these characters can be seen apparently from the Eq. (3). Therefore, for the fixed distance, the final flux would excess the point source sensitivity of *Fermi* for the larger UCMHs mass or smaller dark matter mass. On the other hand, it is also can be seen from the Eq.(3) that the final flux also depends on the decay channels while the difference are not very large [9]. Moreover, one should realize that integrated flux have relation with the dark matter decay rate and which

---

[2] http://www.physto.se/ edsjo/darksusy/

[3] http://fermi.gsfc.nasa.gov/science/instruments /table1-1.html

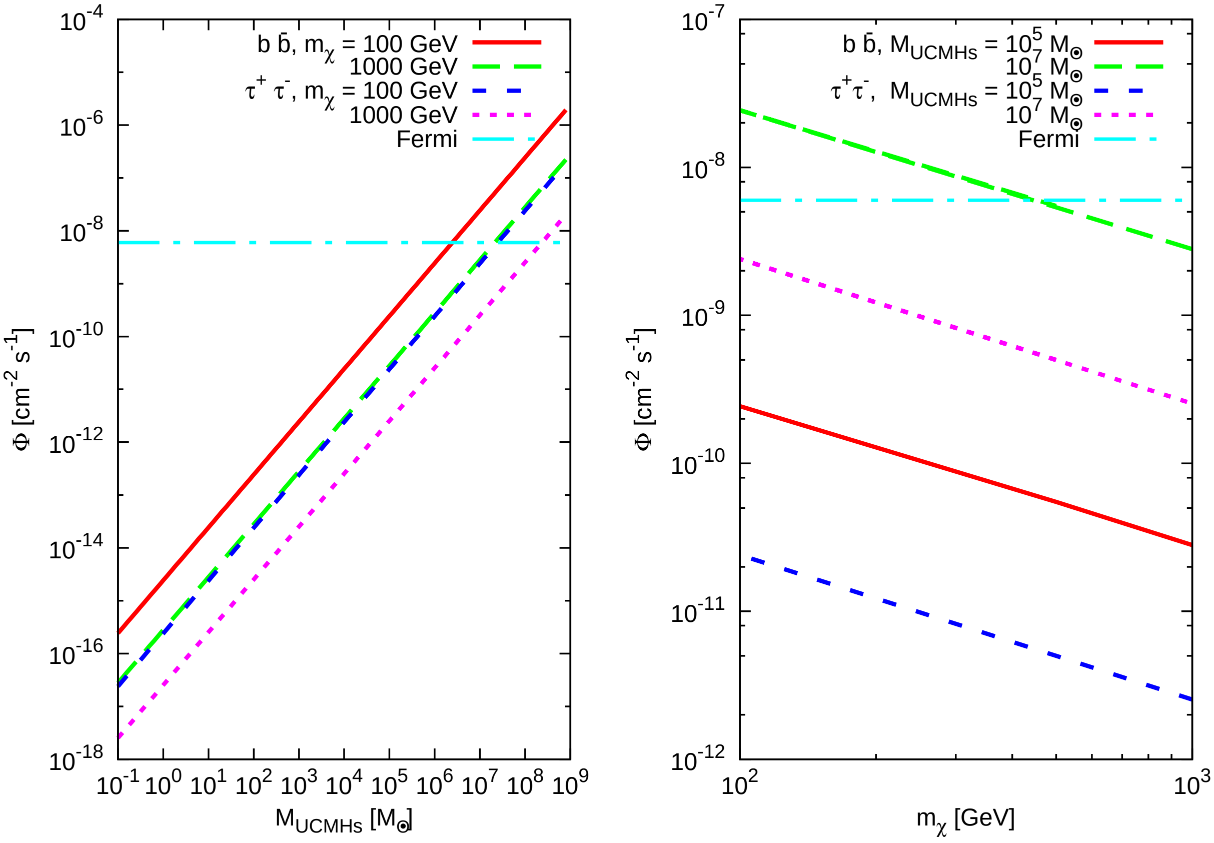

FIG. 1: The integrated γ-ray signals above 0.1GeV from nearby UCMH ($d = 10$kpc) due to dark matter decay. Two decay channels are shown: $b\bar{b}$ and $\tau^+\tau^-$ and the decay rate is $\Gamma = 10^{-26}s^{-1}$. The point source sensitivity of *Fermi* are also shown.

now have been constrained by many observations [14–20].

III. CONSTRAINTS ON THE FRACTION OF UCMHS

Following the method in Ref. [8], the fraction of UCMHs can be defined as

$$f_{\mathrm{UCMHs}} = \frac{\mathrm{M_{UCMHs}}(z=0)}{\mathrm{M_{DM}}(r < d_{obs})} \tag{4}$$

where d_{obs} is the distance that the γ-ray signals from UCMHs would be observed by the detector and $\mathrm{M_{DM}}(r < d_{obs})$ is the mass of Milky Way within these radius. We use three kinds of density profile for the Milky Way, NFW, Isothermal, Einasto and use the value of parameters following the Ref. [18]. We also assume that the abundance of UCMHs is same everywhere [7, 9].

From the discussions in section 2, it can be seen that several parameters can effect the final integrated γ-ray flux. So the final constraints on the abundance of UCMHs will be effected by these parameters. In this section, we will discuss in detail how these parameters effect the final constraints. One of the important parameters is the dark matter decay rate (Γ). It has no defined theoretical value but has to be constrained by observations. There are many ways to give the constraints on this parameter including through the extragalactic γ-ray background or CMB. In this work, we use the WMAP-7 years data to get the constraints on the decay rate. The detail discussions of effect of dark matter decay on the CMB one can see the Ref. [21]. Here we only give the general description. The dark matter can decay into the standard particles such as photons (γ), electrons (e^-) and positrons (e^+) and so on. These decay particles will have interaction with the content of cosmology, such as the interaction between the photons and the hydrogen atoms which formed during the recombination ($z \sim 1100$). One of the effect is to delay the recombination. Moreover, the dark matter decay would be one kinds of sources of reionization ($z < 10$). All of these effect will influence the power spectrum of CMB and we can use the WMAP data to get the constraints on the decay rate. Following the method in Refs. [21, 22], we also used the parameter $\zeta\Gamma$ which describe the dark matter decay and ζ stands for the energy fraction which have injected into the baryonic gas by the dark matter decay. In order to get the constraints, we use the seven years WMAP data [23], and the data from ACBAR [24], Boomerang [25], CBI [26] and VSA [27] experiments and 7 cosmological parameters, where $\Omega_b h^2$ and $\Omega_d h^2$ are the density of baryon and dark matter, θ is the ratio of the sound horizon at recombination to its angular diameter distance multiplied by 100, τ is the optical depth, n_s is the spectral index and A_s is the amplitude of the primordial density perturbation power spectrum. We modified the public code CAMB [4] to include the effect of dark matter decay and the code COSMOMC [5] to get the constraints on parameters. The final results are listed in Tab. I. From these results, we can get the constraints on the decay rate for the WMAP-7 years: $\zeta\Gamma < 0.77 \times 10^{-25} s^{-1} (2\sigma)$. Generally speaking, ζ depends on the redshift and different decay channels. In the following work, we set $\zeta = 1$ and it is enough for our

---

[4] http://camb.info/

[5] http://cosmologist.info/cosmomc/

TABLE I: Posterior constraint on cosmological parameters including dark matter decay from WMAP-7 years observation.

.

Parameters	$100\Omega_b h^2$	$\Omega_c h^2$	θ_S	τ	$\Gamma(\times 10^{-24})$	n_s	$\log[10^{10} A_s]$
Mean	2.231	0.119	1.040	0.075	0.035	0.958	3.113
2σ lower	2.143	0.113	1.036	0.042	0.000	0.937	3.050
2σ upper	2.321	0.125	1.104	0.105	0.077	0.980	3.178

consideration.

For the decay channels, we consider $b\bar{b}$, W^+W^-, $\tau^+\tau^-$ and $\mu^+\mu^-$. The lepton channels are favored by the observations of positrons by PAMELA [17, 28–30] and ATIC [31, 32]. The final constraints on the fraction of UCMHs for different dark matter mass, decay channels and density profile are shown in Figs. 2, 3, 4. From these figures, it is can be seen that the strongest constraints comes from the $b\bar{b}$ channel and the dark matter mass $\mathrm{m}_\chi = 100\mathrm{GeV}$. The corresponding fraction is $\mathrm{f_{UCMHs}} \sim 5\times 10^{-5}$ with the mass of UCMHs $\mathrm{M_{UCMHs}} \sim 10^6 \mathrm{M}_\odot$. The results of W^+W^- channel are comparable with the $b\bar{b}$ case. For the mass of UCMHs smaller than $\sim 10^6 \mathrm{M}_\odot$, the constraints are similar for different density profile. The obvious difference come from the larger mass $\mathrm{M_{UCMHs}} > 10^6 \mathrm{M}_\odot$. The corresponding distance is longer for these larger mass and the changes of mass within these radius are slow for the Isothermal density profile. So the increase of fraction for these mass range is gently for the Isothermal model. For the fixed mass of dark matter and UCMHs, the constraints for the lepton decay channels are weaker. This is due to the smaller integrated photon number for these decay channels. It is also can be seen that the constraints in this work are weaker than the other works which considered the dark matter annihilation case [8, 9]. The main reason is that the strength of ark matter decay is proportional to the density but not to the density square.

The constraints on fraction of UCMHs plotted in Figs. 2, 3 and 4 can be fitted in a simple form for the mass range $\mathrm{M_{UCMHs}} \sim 10^{-4} - 10^{14} \mathrm{M}_\odot$

$$\mathrm{Y} = \mathrm{a}(\mathrm{X}-\mathrm{b})^2 + \mathrm{c}(\mathrm{X}-\mathrm{d})^3 + \mathrm{e}(\mathrm{X}-\mathrm{f})^4. \tag{5}$$

where $\mathrm{Y} = \log_{10}\mathrm{f_{UCMHs}}$, $\mathrm{X} = \log_{10}\mathrm{M_{UCMHs}}$ and the value of parameters are shown in Tab. II.

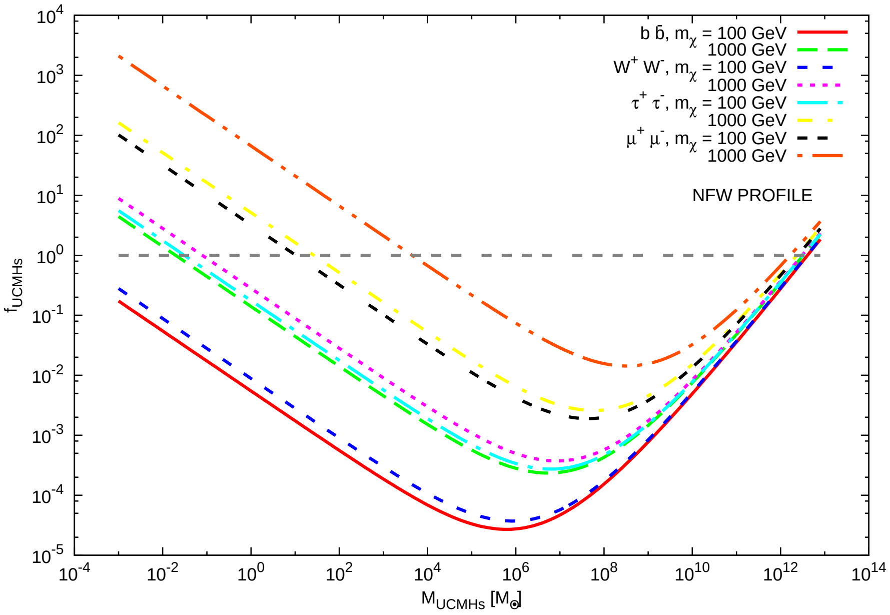

FIG. 2: Constraints on the fraction of UCMHs for different dark matter mass and decay channels. Here the NFW density profile and four decay channels $b\bar{b}$, W^+W^-, $\tau^+\tau^-$ and $\mu^+\mu^-$ are used. We have chosen two values of dark matter mass $m_\chi = 100$ and 1000GeV.

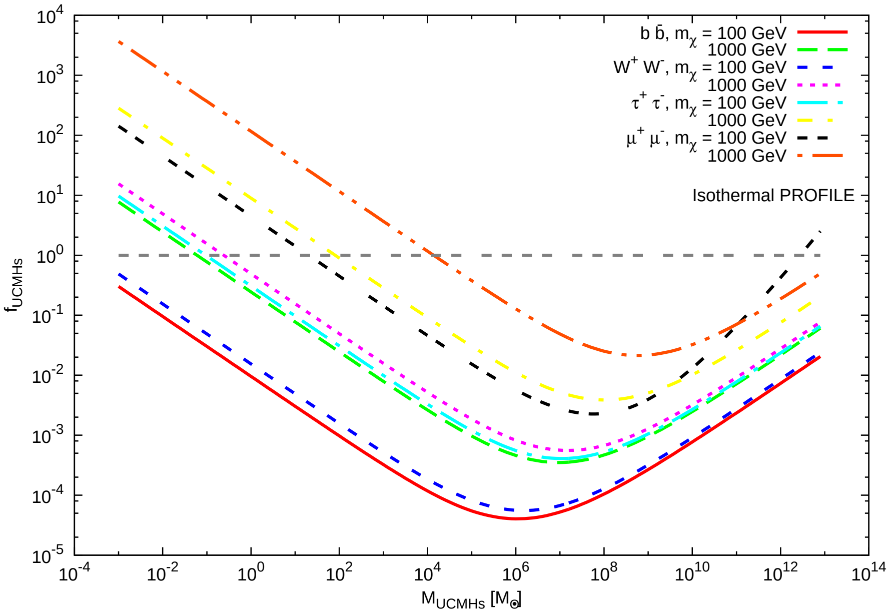

FIG. 3: Constraints on the fraction of UCMHs. The dark matter mass and decay channels are the same with Fig. 2 but the Isothermal density profile.

IV. CONCLUSIONS

It is excepted that the UCMHs would contribute the γ-ray flux as its high density due to the dark matter decay within them. On the other hand, the abundance of UCMHs is very important for the constraints on the primordial density perturbations of smaller scale. In this work, we investigated the integrated γ-ray flux from nearby UCMHs due to the dark matter decay. For the larger mass of UCMHs or smaller dark matter mass, e.g. $\mathrm{m}_\chi = 200\mathrm{GeV}$, $\mathrm{M}_{\mathrm{UCMHs}} = 10^7 M_\odot$ and $b\bar{b}$ decay channel, the integrated γ-ray flux would achieve the point source sensitivity of $Fermi$. We mainly researched the influence of different parameters and density profile of Milky Way on the constraints of UCMHs abundance. One of the important parameters is the dark matter decay rate (Γ). Because the cosmological evolution, e.g. reionization, can be effected by the dark matter decay, so this parameter can be constrainted by the CMB observations. In this work, we used the WMAP-7 years data to get the constraint and used that result to do the following calculations. We considered four decay channels: $b\bar{b}$, W^+W^-, $\tau^+\tau^-$ and $\mu^+\mu^-$, and assumed the branch ratio of each channel $B_f = 1$. For the density profile of dark matter halo of Milk Way, we used NFW,

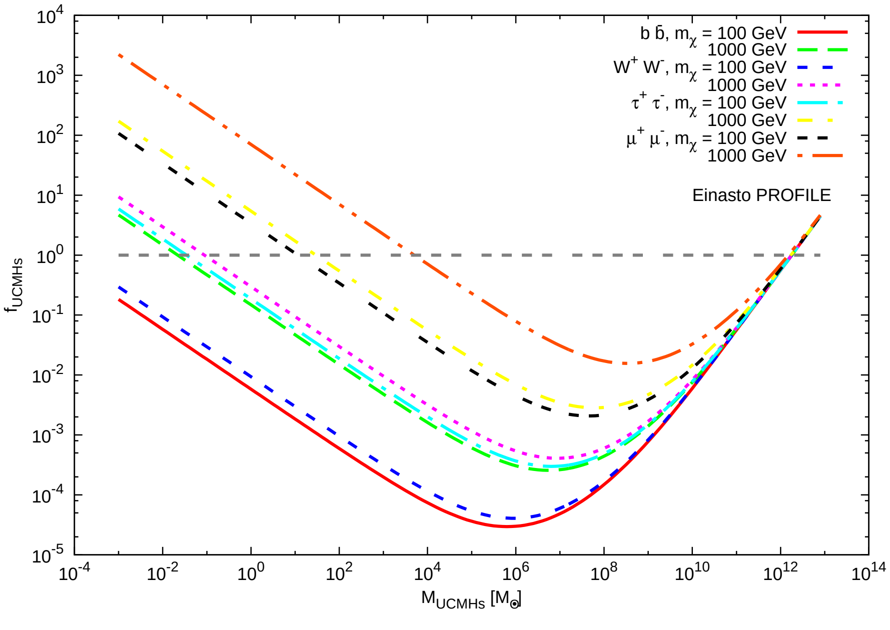

FIG. 4: Constraints on the fraction of UCMHs. The dark matter mass and decay channels are the same with Figs. 2 and 3 but the Einasto density profile.

TABLE II: Constraints on the fraction of UCMHs in the form $\mathrm{Y = a(X-b)^2 + c(X-d)^3 + e(X-f)^4}$ where $\mathrm{Y = log_{10} f_{UCMHs}}$ and $\mathrm{X = log_{10} M_{UCMHs} (M_{UCMHs} = 10^{-4} \sim 10^{14} M_{\odot})}$.

Parameters	$b\bar{b}(100GeV)$	$b\bar{b}(1TeV)$	$W^+W^-(100GeV)$	$W^+W^-(1TeV)$	$\tau^+\tau^-(100GeV)$	$\tau^+\tau^-(1TeV)$	$\mu^+\mu^-(100GeV)$	$\mu^+\mu^-(1TeV)$
(NFW)a	0.13956	-0.15256	-0.03859	-0.14354	-0.15274	-0.20274	-0.14974	-0.29913
b	-3.64829	-2.49367	-7.00440	-2.17802	-2.37304	-3.98168	-7.72446	-3.86850
c	0.03344	0.01851	0.02043	0.01585	0.01709	-0.00576	-0.00013	-0.01101
d	-1.14816	-2.41174	-0.85531	-2.09851	-2.27138	2.70978	7.84879	1.92213
e	-0.00053	-0.00039	-0.00050	-0.00033	-0.00038	0.00015	0.00005	0.00022
f	-9.36757	-3.71259	-3.65879	-2.88512	-2.86262	-12.55640	-20.9078	-12.94170
(Isothermol)a	-0.04872	-0.14664	-0.05287	-0.12266	0.00300	-0.05541	-0.08184	-0.06133
b	-6.38399	-2.26827	-5.78171	-2.04697	30.66510	18.28760	18.28740	18.28440
c	0.00906	0.01450	0.01262	0.01224	-0.001332	-0.00636	-0.00885	-0.00669
d	-1.27286	-2.19990	-1.00770	-1.80317	-17.00310	-62.62520	-62.62000	-62.52440
e	-0.00046	-0.00042	-0.00044	-0.00031	0.00005	0.00003	0.00004	0.00003
f	0.96076	-1.33955	-1.14492	-1.19346	-15.88920	-87.5285	-87.5319	-87.59300
(Einasto)a	-0.07591	-0.06893	-0.04353	-0.07389	-0.07079	-0.08623	-0.08519	0.01641
b	18.30970	18.30020	18.31810	18.28830	18.27540	18.26390	18.2667	11.18760
c	-0.00878	-0.00813	-0.00621	-0.00848	-0.00825	-0.00922	-0.00918	-0.00627
d	-62.80660	-62.77580	-63.02030	-62.74770	-62.79310	-62.64560	-62.66000	-4.4091
e	0.00004	-0.00003	0.00003	0.00004	0.00004	0.00004	0.00004	0.00025
f	-87.38460	-87.42290	-87.24350	-87.46820	-87.47360	-87.58250	-87.56880	-6.13439

Isothermal and Einasto models to get the final constraints. We found that the strongest constraints on the fraction of UCMHs comes from the smaller dark matter mass and the $b\bar{b}$ channel $\mathrm{f_{UCMHs}} \sim 5 \times 10^5$ for $\mathrm{M_{UCMHs}} \sim 10^6 \mathrm{M_\odot}$. For these three kinds of density profile, the strongest constraints are similar. The obvious differences come from the larger UCMHs mass $\mathrm{M_{UCMhs}} > 10^6 \mathrm{M_\odot}$. It can be considered as the difference of the changes of mass within the corresponding radius for the different density profile.

Acknowledgments

Our MCMC chains computation was performed on the Shenteng 7000 system of the Supercomputing Center of the Chinese Academy of Sciences.

---

[1] A. M. Green and A. R. Liddle, *Phys. Rev. D* **56** (1997) 6166.

[2] M. Ricotti and A. Gould, *Astrophys. J.* **707** (2009) 979.

[3] Y. Yang, X. Huang, X. Chen and H. Zong, *Phys. Rev. D* **84** (2011) 043506.

[4] Y. Yang, X. Chen, T. Lu and H. Zong, *Eur. J. Phys. Plus* **126** (2011) 123.

[5] D. Zhang, *MNRAS* **418** (2011) 1850.

[6] Y. Yang, L. feng, X. Huang, X. Chen, T. Lu and H. Zong, *JCAP* **12** (2011) 020.

[7] P. Scott, S. Sivertsson and S. Sivertsson, *Phys. Rev. Lett.* **103** (2009) 211301.

[8] A. S. Josan and A. M. Green, *Phys. Rev. D* **82** (2010) 083527.

[9] T. Bringmann, P. Scott and Y. Akrami, *Phys. Rev. D* **85** (2012) 125027.

[10] F. Li, A. L. Erickcek and N. M. Law, arXiv: 1202.1284

[11] J. A. Fillmore and P. Goldreich, *Astrophys. J.* **281** (1984) 1.

[12] E. Bertschinger, *Astrophys. J. Suppl.* **58** (1985) 39.

[13] E. Komatsu et al, *Astrophys. J. Suppl.* **192** (2011) 18.

[14] M. Cirelli, E. Moulin, P. Panci, P. D. Serpico and A. Viana, arXiv:1205.5283.

[15] L. Dugger, T. E. Jeltema and S. Profumo, *JCAP*, **12** (2010) 015.

[16] L. Zhang, C. Weniger, L. Maccione, J. Redondo and G. Sigl, *JCAP*, **06** (2010) 027.

[17] A. Ibarra, D. Tran and C. Weniger, *JCAP*, **1001** (2010) 009.

[18] M. Cirelli, P. Panci, P. D. Serpico, *Nucl. Phys. B*, **840** (2010) 284.

[19] G. Bertone, W. Buchmuller, L. Covi and A. Ibarra, *JCAP*, **0711** (2007) 003.

[20] G. Hutsi, A. Hektor and M. Raidal, *JCAP*, **7** (2010) 8.

[21] X. Chen and M. Kamionkowski, *Phys. Rev. D*, **70** (2004) 043502.

[22] L. Zhang, X. Chen, M. Kamionkowski, Z. Si and Z. Zheng, *Phys. Rev. D*, **76** (2007) 061301.

[23] L. Dunkely et al, , (0803.0586)

[24] C. L. Kuo et al, *Astrophys. J.*, **664** (2007) 687.

[25] T. E. Montroy et al, *Astrophys. J.*, **647** (2006) 813.

[26] A. C. S. Readhead et al, *Astrophys. J.*, **609** (2004) 498.

[27] C. L. Kuo et al, *Mon. Not. Roy. Astron. Soc.*, **353** (2004) L732.

[28] O. Adriani et al, *Nature*, **458** (2009) 607.

[29] A. Ibarra and D. Tran, *JCAP*, **0902** (2009) 021.

[30] A. Ibarra and D. Tran, *Phys. Rev. D*, **79** (2009) 023512.

[31] J. Chang et al, *Nature*, **456** (2008) 362.

[32] J. Liu, P. Yin and S. Zhu, *Phys. Rev. D*, **79** (2009) 063522.